Indian J. Met. Hydrol. Geophys. (1978), **29**, 1 & 2, 260-272

551·553·21 : 551·515·1

Diagnostic study of a monsoon depression

K. V. RAO and G. S. P. RAO

Meteorological Office, Pune

and

S. RAJAMANI

Indian Institute of Tropical Meteorology, Pune

ABSTRACT. The entire life cycle of an intense monsoon depression which formed during the ISMEX period of 1973 was investigated by making use of the quasi-geostrophic baroclinic model. Vertical and meridional profiles of the vorticity associated with the system are presented. Large-scale vertical velocity computed by the ω-equation is also discussed. The kinetic and potential energies and the various energy conversion terms have been evaluated. The flow diagrams relating to the energy conversion terms show that the energy conversions take place in the proper direction.

Radiosonde data from Soviet ships between Lat. 8°N and 12°N have enabled the detection of a closed low between 500 and 300 mb near about 10°N and 65°E. Vertical profiles of geostrophic vorticity and vertical velocity associated with this system are also discussed.

1. Introduction

In their earlier investigations making use of quasi-geostrophic baroclinic model, Rao and Rajamani (1970, 1972a, 1972b and 1975) studied some of the features of the monsoon depressions by making computations corresponding to a particular synoptic hour on a single day. In this paper, they have extended the study to cover the entire life cycle of a depression. During the period 16 May to 11 July 1973, the Indo-Soviet Monsoon Experiment was arranged and it was hoped that the data coverage during that period would be adequate for such a detailed study, and so the case of a deep depression during July 1973 was selected.

2. Synoptic situation

2.1. *Bay of Bengal system*

There was a well marked low pressure area over northwest Bay of Bengal and adjoining west-central Bay, at 03 GMT on 4 July. This low developed into a depression at 03 GMT of the next day with its centre near 19·5°N and 88°E. It intensified further into a deep depression by 12 GMT of 6 July with its centre near 20·5°N and 86·5°E. Moving rather slowly, it was close to Orissa coast on the morning of 7 July and crossed the coast that evening. It was centred near Champa (22°N, 83°E) at 03 GMT of 8 July and continued to be deep depression. By 03 GMT of 9 July, it had weakened into a depression with its centre at Narsinghpur (23°N, 79°E).

Synoptic charts of 1000, 850, 500, 300 and 200 mb levels were prepared for 12 GMT of 4 to 8 July 1973 and from the analysed charts, the contour heights of all the standard isobaric levels were picked up at grid points at the intersections of 2° latitudes and longitudes. The area of analysis extends from 6° to 26°N and from 56° to 100°E.

In Fig. 1 are represented, the synoptic charts of 6 July, when the system had intensified into a deep depression.

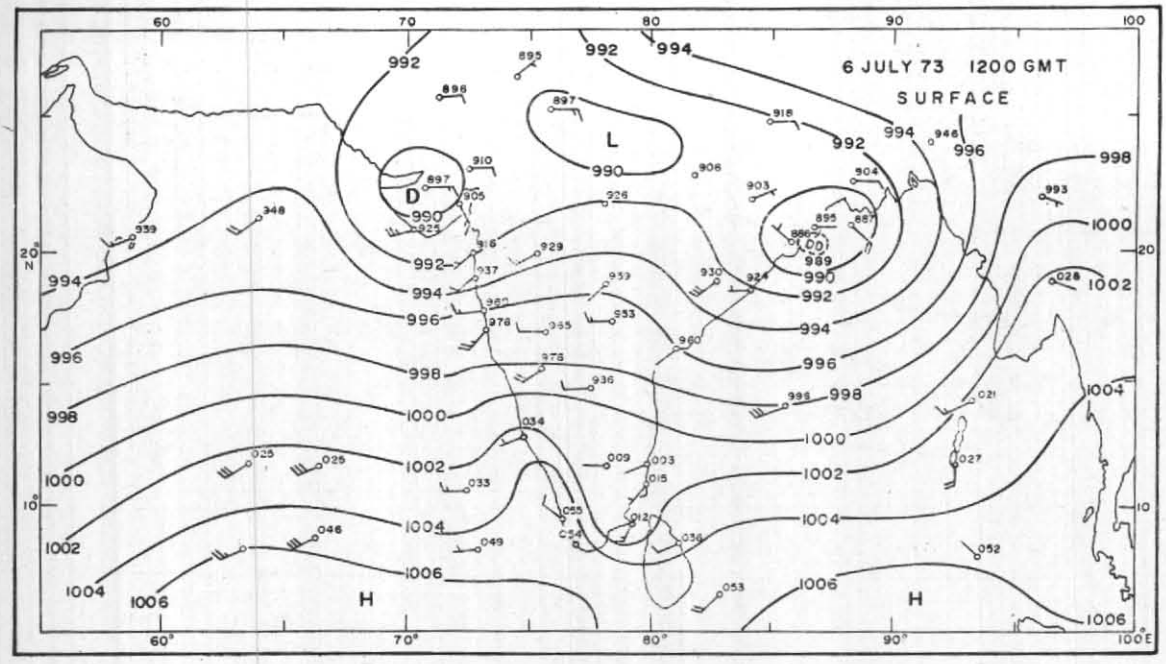

Fig. 1(a). Surface chart for 1200 GMT of 6 July 1973

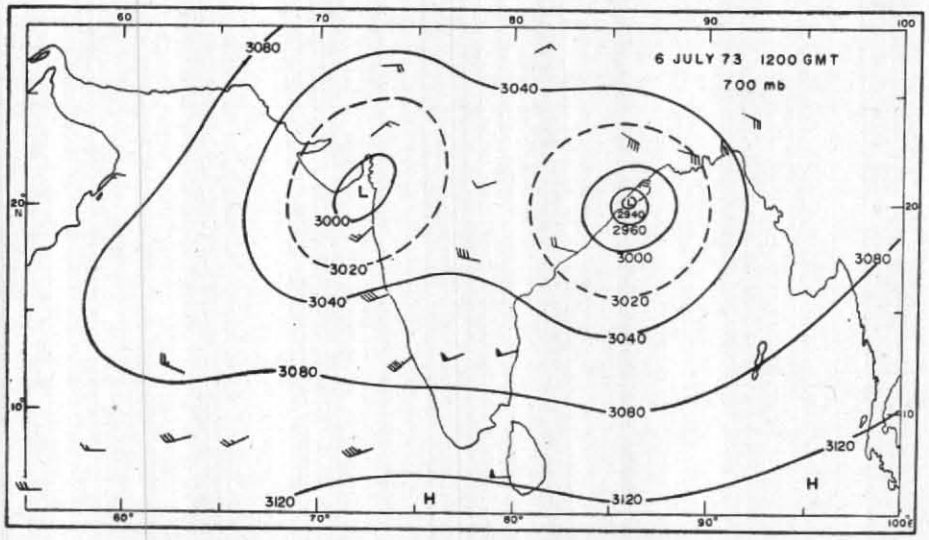

Fig. 1(b). 700 mb level chart for 1200 GMT of 6 July 1973

2.2. *West Arabian system*

Although our expectation of the larger coverage of data in the field of monsoon depression was not realised, radiosonde and wind data became available for the first time at various levels in the region 60° to 75°E and 8° to 12°N from four Soviet ships, ***Okion***, ***Voeykov***, ***Priliv*** and ***Shoklasky***. These data have revealed an interesting result. As can be seen from Fig. 1 there was a closed circulation system at 300 mb around 10°N and 65°E over west Arabian Sea. This system was present between 500 and 300 mb levels only and was not seen in the lower levels, The locations of the system at 300 mb level on 4 and 7 July are given in Fig. 2.

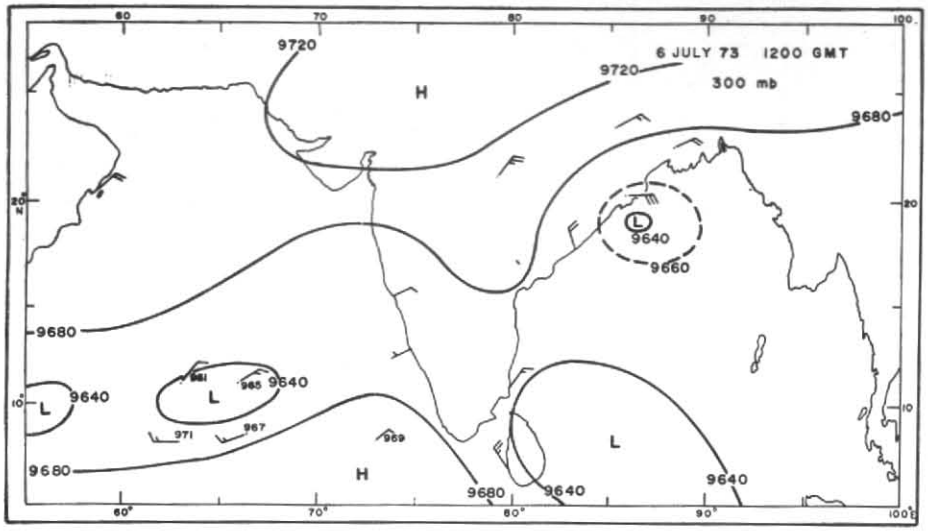

Fig. 1(c). 300 mb level chart for 1200 GMT of 6 July 1973

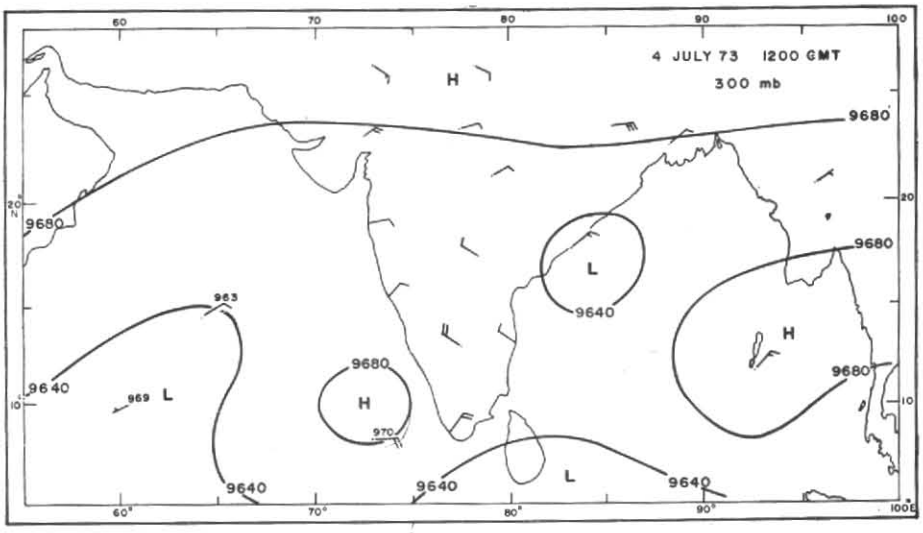

Fig. 2(a). 300 mb level chart for 1200 GMT of 4 July 1973

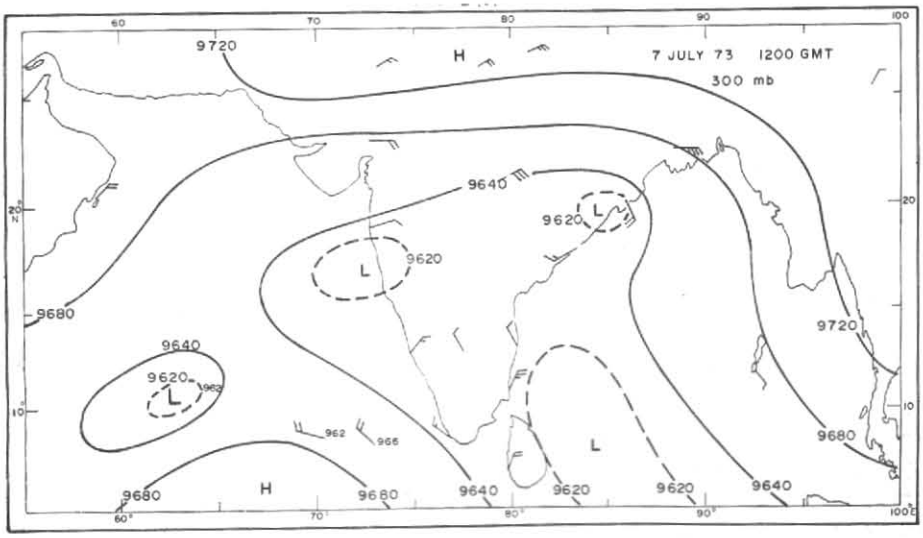

Fig. 2(b). 300 mb level chart for 1200 GMT of 7 July 1973

3. Computation

3.1. *Equations*

The equations used in this study are as follows:

The quasi-geostrophic vorticity equation is given by

$$\frac{\partial \zeta}{\partial t} + \mathbf{V}.\nabla(\zeta + f) = f_0 \frac{\partial \omega}{\partial p} \quad (1)$$

(Refer Appendix I for explanation of symbols)

The thermodynamic energy equation for adiabatic motion is given by

$$\frac{\partial}{\partial t}\left(\frac{\partial \phi}{\partial p}\right) + \mathbf{V}.\nabla\left(\frac{\partial \phi}{\partial p}\right) + \sigma\omega = 0 \quad (2)$$

where σ is the static stability given by the relation

$$\sigma = -\alpha \frac{\partial}{\partial p} (\ln \theta)$$

Using equations (1) and (2), the ω-equation given below is obtained.

$$\sigma \nabla^2 \omega + f_0^2 \frac{\partial^2 \omega}{\partial p^2} = f_0 \frac{\partial}{\partial p}\left[\mathbf{V}.\nabla(\zeta + f)\right] - \nabla^2\left[\mathbf{V}.\nabla\left(\frac{\partial \phi}{\partial p}\right)\right] \quad (3)$$

3.2. *Bay of Bengal system*

The vertical cross section of geostrophic relative vorticity along 20°N for 4, 5, 6, 7 and 8 July are presented in Fig. 3.

The interesting point to note is that during 5 to 7 July the cyclonic vorticity values are large in a narrow vertical column between grid points 84°E and 88°E reaching maximum values between 700 and 300 mb levels.

The meridional profile along 86°E of the absolute vorticity for the period 4th to 8th is given in Fig. 4. On 5th, 6th and 7th, the maximum value is located at 20°N and 86°E. It may be mentioned that the monsoon depressions form over the head Bay of Bengal, near about 20°N.

The vertical profile of geostrophic relative vorticity at a grid point where the value is maximum is presented in Fig. 5. It is seen that from 4 to 7 July, the vorticity increases with height reaching a maximum value at 700 mb level except on 4th and 7th when the maximum value is at 500 mb level. On 6 July, the maximum value of 9×10^{-4} per sec is at 700 mb level.

During the stage of intensification of the system it is seen that there is large increase between 850 and 500 mb levels from 4 to 6 July. In order to understand how the large increase in vorticity is brought about, the magnitudes of the various terms in the equation for the local rate of change of vorticity are computed.

$$\frac{\partial \zeta}{\partial t} = -\mathbf{V}.\nabla(\zeta + f) - \omega \frac{\partial \zeta}{\partial p} - (\zeta + f)\nabla.\mathbf{V} - \nabla\omega.\frac{\partial \mathbf{V}}{\partial p} \times \mathbf{k} \quad (4)$$

The magnitudes of the various terms at 700 mb level for the grid point 20°N, 84°E are presented in Table 1.

The computations show that between the longitude 84° and 86°E where the system is located during these days, the magnitude of the horizontal advection of vorticity term is one order of magnitude greater than the other terms in the equation. This finding seems to suggest that the intensification of the system is mainly brought about by the advection term of the vorticity equation.

3.3. *Vertical velocity profile*

Eqn. (3) is made use of for computing vertical velocity at the standard isobaric levels, *viz.*, 850 700, 500 and 300 mb levels. The vertical cross sections along 20°N on 5 to 8 July are presented in Fig. 6. On 6th, the maximum value of about 60×10^{-4} mb/sec was obtained for upward vertical velocity at 850 and 700 mb levels. This value, which was nearly 6 cm/sec for large scale vertical velocity, was fairly high, but the system was at its most intense phase at that time.

3.4. *Low latitude Arabian Sea system*

The vertical profile of the geostrophic relative vorticity at the grid points in the location of the system is presented in Fig. 7. This brings out clearly that the positive vorticity associated with this system is present between the levels 700 and 200 mb reaching a maximum value at 300 mb on 4, 5, 6 and 7 July and at 500 mb on 8 July. Apart from the fact that a closed system could be drawn with contour heights and wind values at the location of the few ships, the satellite cloud pictures also suggest the presence of a closed system at these higher levels. The vertical profile of the vertical velocity at a grid point where the value is maximum over the low latitude Arabian Sea system

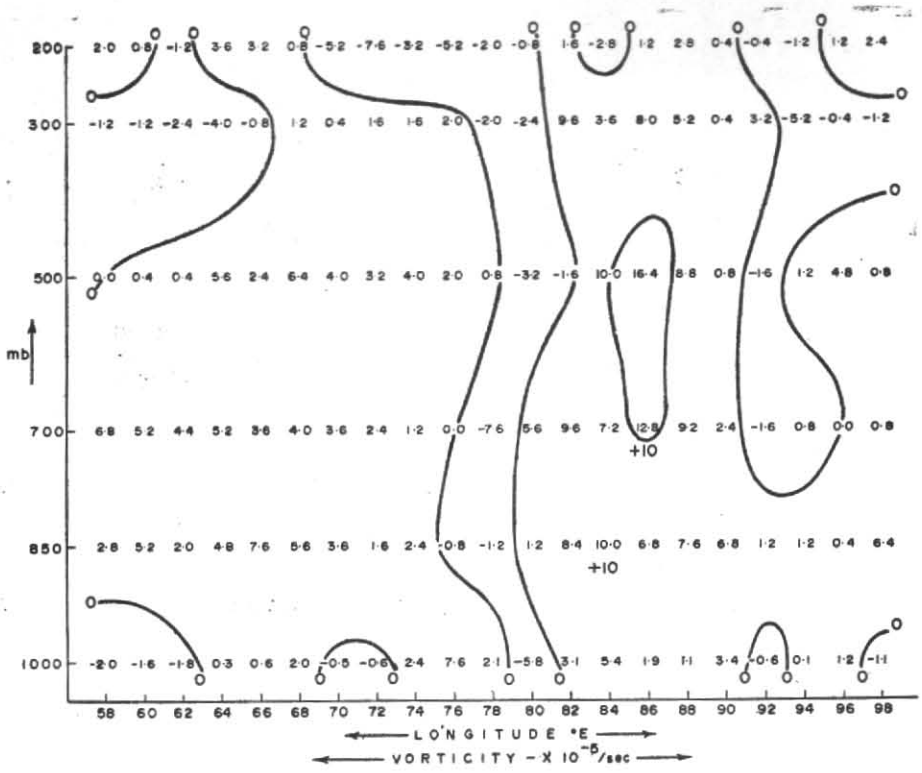

Fig. 3(a). Geostrophic relative vorticity along latitude 20°N on 4 July 1973, 1200 GMT

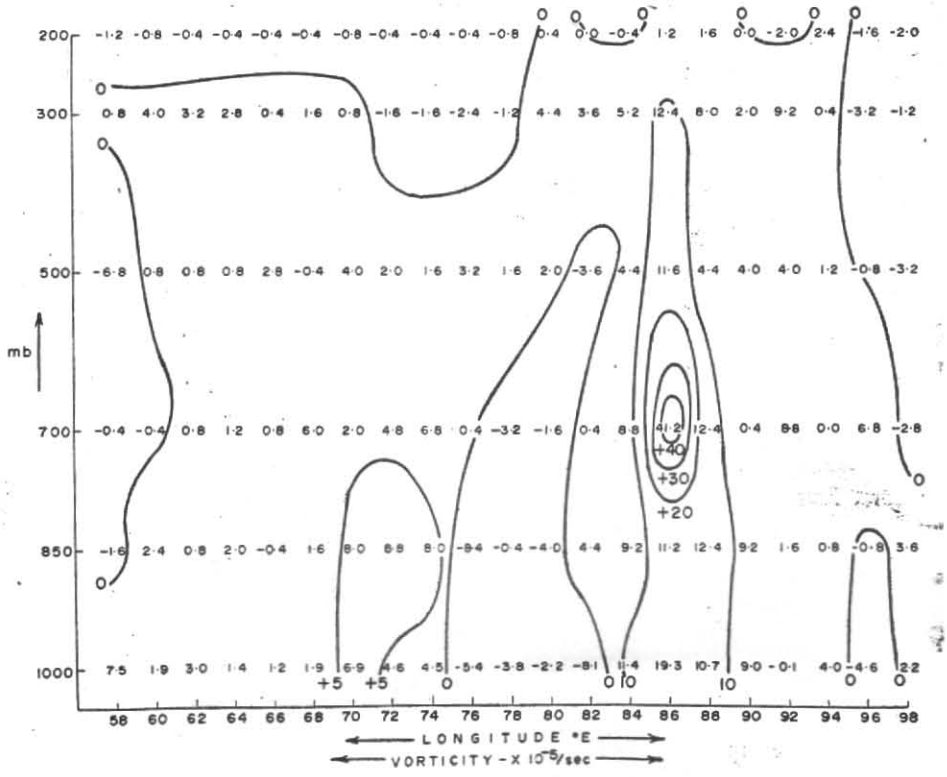

Fig. 3(b). Geostrophic relative vorticity along latitude 20°N on 5 July 1973, 1200 GMT

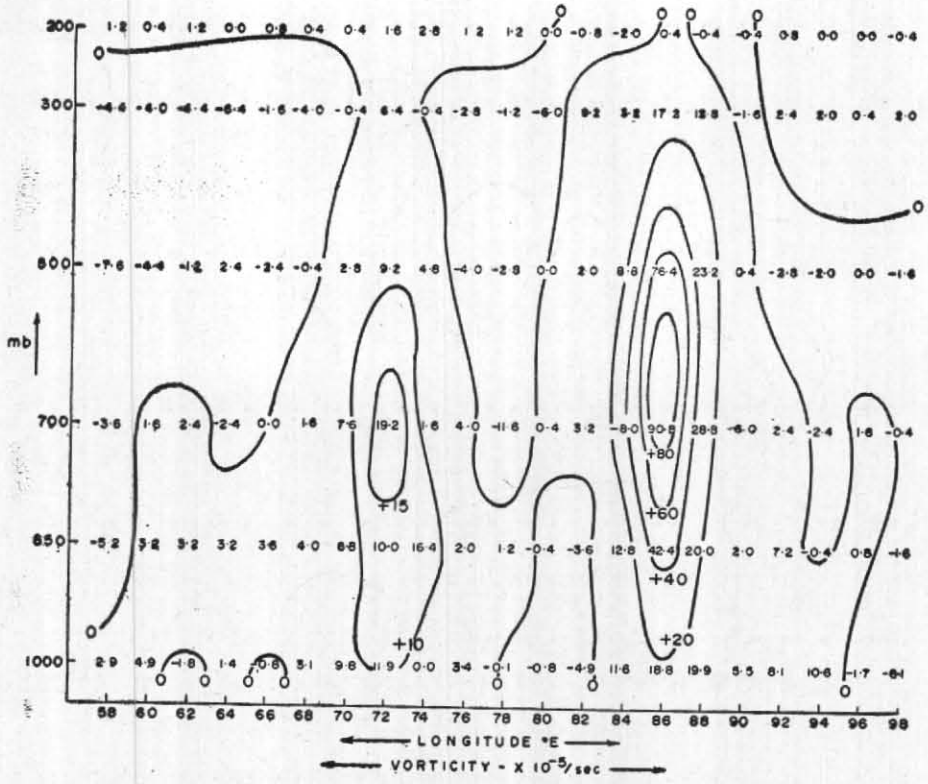

Fig. 3(c). Geostrophic relative vorticity along latitude 20°N on 6 July 1973, 1200 GMT

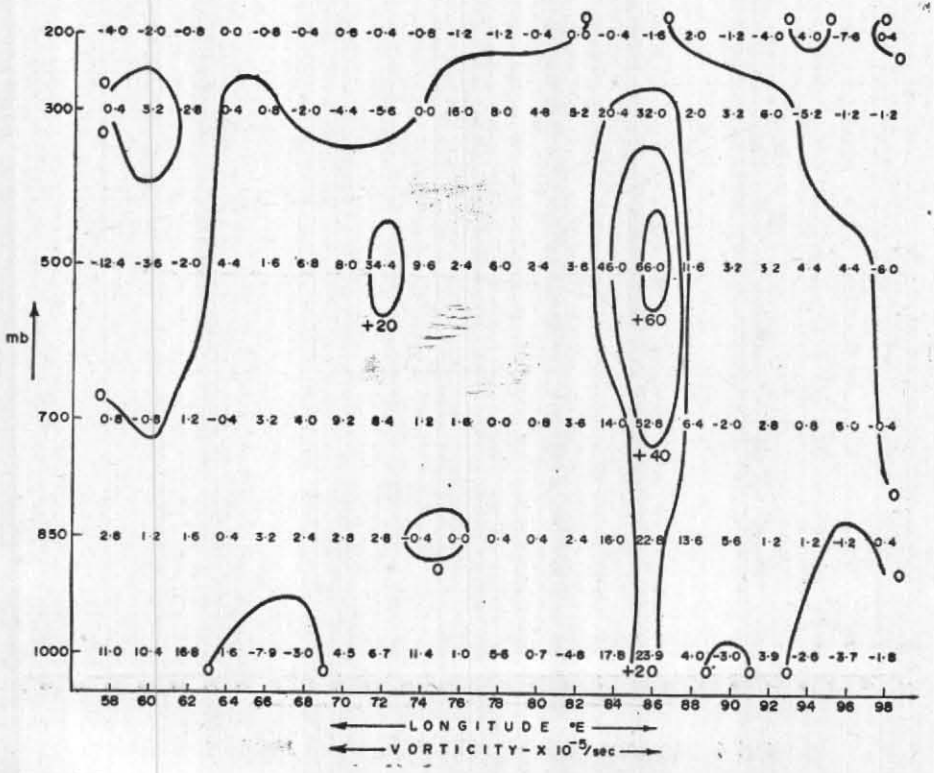

Fig. 3(d). Geostrophic relative vorticity along latitude 20°N on 7 July 1973, 1200 GMT

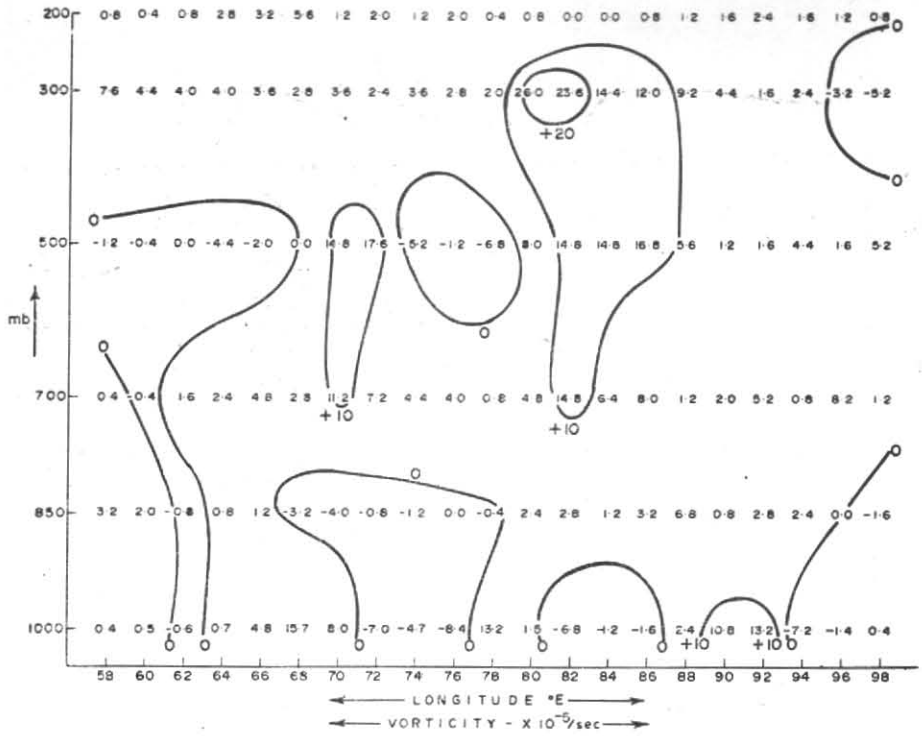

Fig. 3(e). Geostrophic relative vorticity along latitude 20°N on 8 July 1973, 1200 GMT

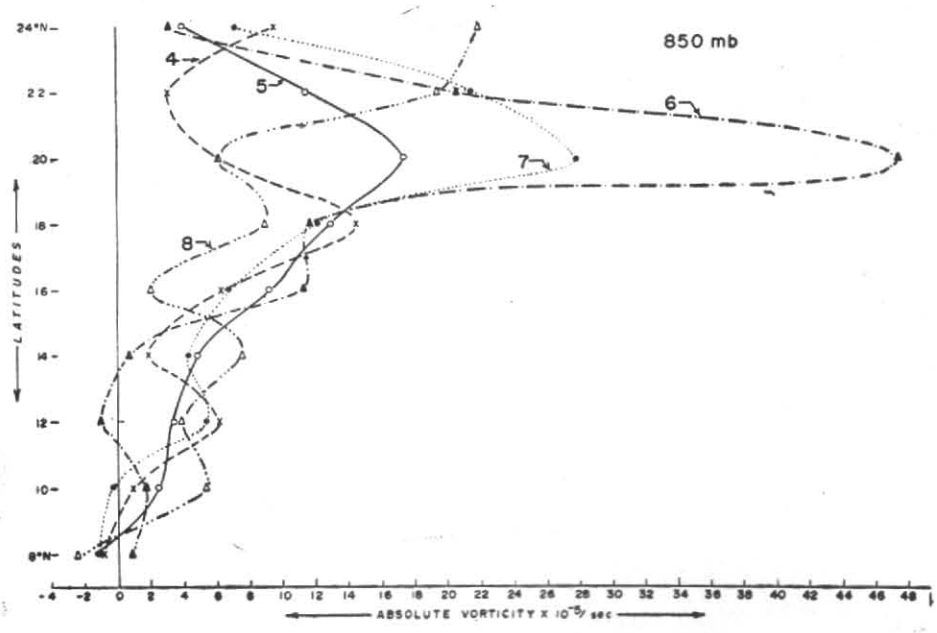

Fig. 4. Absolute vorticity profiles from 4 to 8 July 1973

TABLE 1

Relative vorticity tendency at 20° N and 84° E from 4 to 8 July 1973 1200 GMT

Date (July 73)	$-\mathbf{V}.\nabla(\zeta+f)$	$-\omega\frac{\partial\zeta}{\partial p}$	$-(\zeta+f)\nabla.\mathbf{V}$	$-\nabla\omega.\frac{\partial\mathbf{V}}{\partial p}\times\mathbf{k}$
4	0·4	−0·6	−1·2	2·1
5	9·3	0·0	−3·4	0.5
6	42·7	2·3	1·7	2·9
7	−35·9	−6·7	−10·0	−6·1
8	4·0	−3·9	−6·9	−1·2

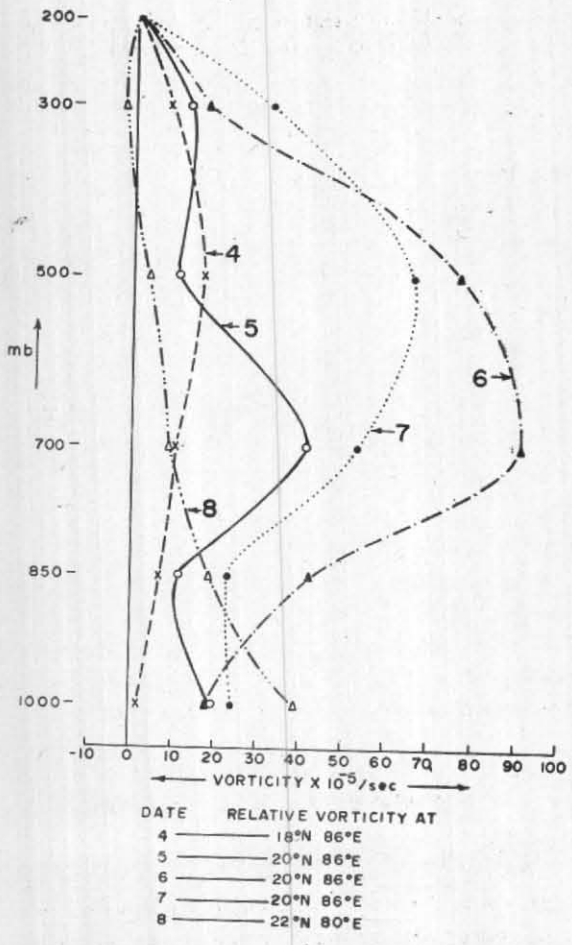

Fig. 5. Vertical profiles of geostrophic relative vorticity at a grid point where the value is maximum over the Bay of Bengal system

for the period from 4 to 8 July is given in Fig. 8. It is seen that the upward vertical velocity of about 3 to 5 mm/sec is present between 850 mb and 300 mb on 5th and between 2 to 4 mm/sec between 850 mb and 500 mb on 6 July.

4. Energetics

In recent years there has been considerable work done by various workers on the subject of energy conversions. Expressions for different energy conversions are derived in Appendix II, following the method of Phillips (1956) and Wiin Nielsen *et al.* (1963). Kinetic energy of the mean zonal motion K_Z and that the perturbation K_E are defined as

$$K_Z = \tfrac{1}{2}\int_M \bar{u}^2\, dm \tag{5}$$

$$K_E = \tfrac{1}{2}\int_M (u'^2 + v'^2)\, dm \tag{6}$$

The available potential energy of the mean zonal motion A_Z and that of the perturbation A_E are

$$A_Z = \frac{1}{2\sigma}\int_M \left(\overline{\frac{\partial\phi}{\partial p}} - \left[\frac{\partial\bar{\phi}}{\partial p}\right]\right)^2 dm \tag{7}$$

$$A_E = \frac{1}{2\sigma}\int_M \left(\frac{\partial\phi}{\partial p} - \overline{\frac{\partial\phi}{\partial p}}\right)^2 dm \tag{8}$$

as defined by Lorenz (1955) and Wiin Nielsen (1965).

All the energy terms K.E. and A.P.E. have been evaluated from geopotential data.

Following Phillips (1956), we adopt the synoptic notation of the form $\{A_Z,K_Z\}$ signifying a transformation from one form — the first in the bracket to the second form.

$$\{A_Z, A_E\} = -\int_M \frac{1}{\sigma}\left(\frac{R}{P}\right)^2 \overline{v'T'}\,\frac{\partial\bar{T}}{\partial y}\, dm \tag{9}$$

$$\{A_Z, K_Z\} = \int_M \bar{\omega}\,\frac{\partial\bar{\phi}}{\partial p}\, dm \tag{10}$$

$$\{A_E, K_E\} = \int_M \overline{\omega'\frac{\partial\phi'}{\partial p}}\, dm \tag{11}$$

$$\{K_E, K_Z\} = -\int_M \overline{u'v'}\,\frac{\partial\bar{u}}{\partial y}\, dm \tag{12}$$

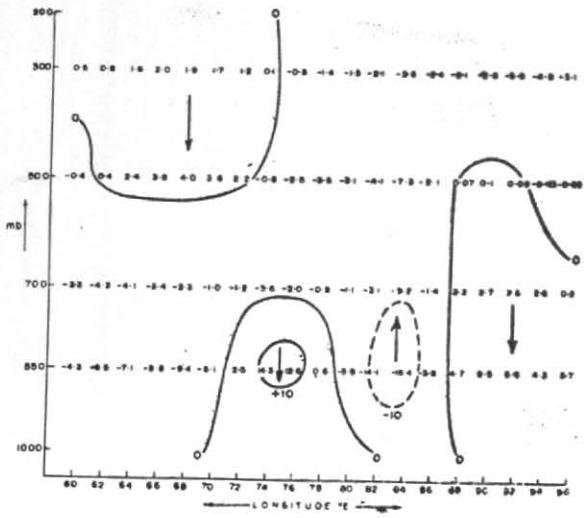

Fig. 6(a). Vertical cross section at latitude 20°N of vertical velocity on 5 July 1973, 1200 GMT

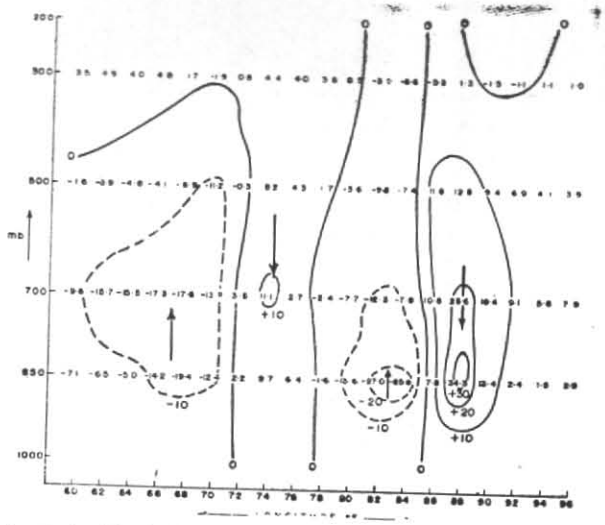

Fig. 6(c). Vertical cross section at latitude 20°N of vertical velocity on 7 July 1973, 1200 GMT

(ω in units of 10^{-4} mb/sec)

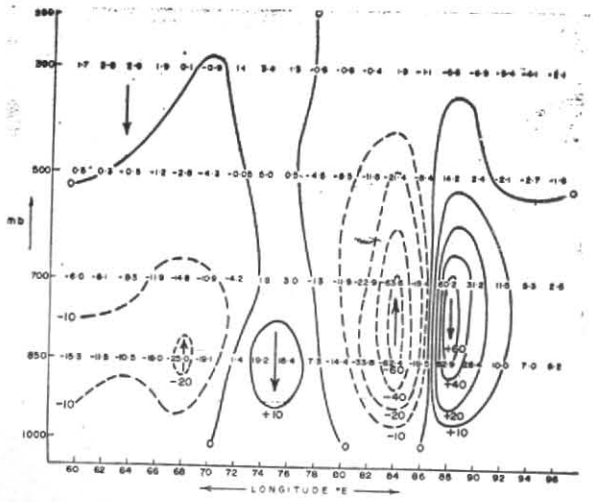

Fig. 6(b). Vertical cross section at latitude 20°N of vertical velocity on 6 July 1973, 1200 GMT

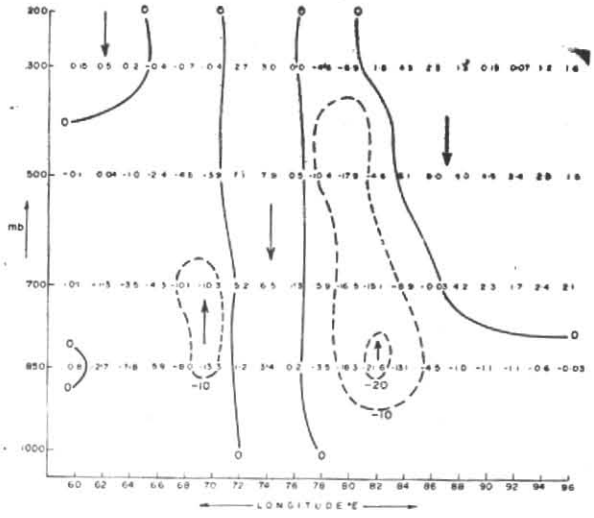

Fig. 6(d). Vertical cross section at latitude 20°N of vertical velocity on 8 July 1973, 1200 GMT

$\{A_Z, A_E\}$ represents a transformation of zonal potential energy to the disturbance (regarded as an eddy) potential energy. This is accomplished by the horizontal transport of sensible heat by the disturbance velocity $v'T'$.

The transformation of zonal potential energy into zonal kinetic energy $\{Az, Kz\}$ represents the effect of vertical circulation in meridional planes $\bar{\omega}(\partial\bar{\phi}/\partial p)$.

The transformation of disturbance potential energy into disturbance kinetic energy $\{A_E, K_E\}$ represents the effect of vertical circulation in zonal planes $\overline{\omega' \frac{\partial \phi'}{\partial p}}$.

The transformation of eddy kinetic energy into the kinetic energy of the mean zonal flow $\{K_E, K_Z\}$ correlates the shear of the mean zonal flow with the mean eddy momentum transport $\overline{u'v'}$.

4.1. *Discussion of results*

Energy terms and conversion of energy terms for a column of one metre square cross section from

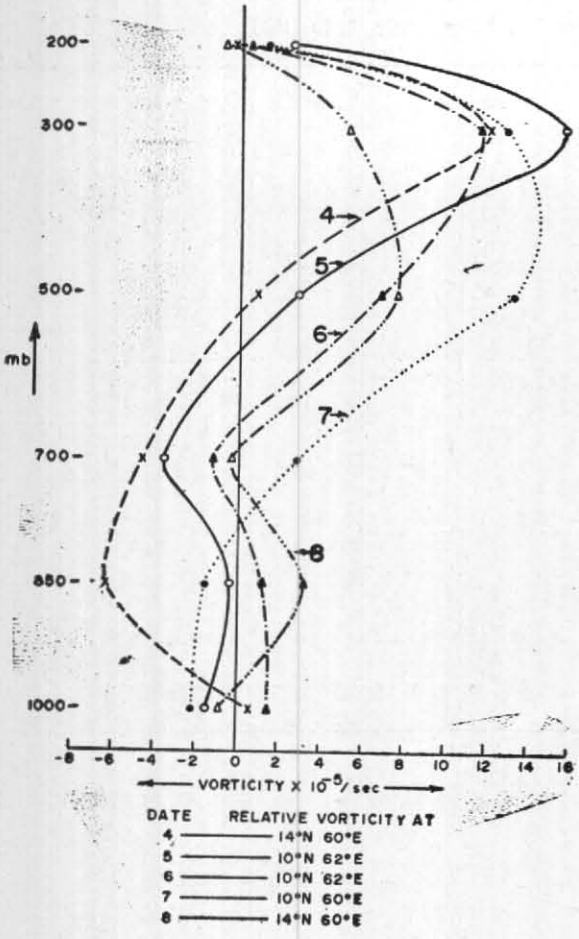

Fig. 7. Vertical profiles for geostrophic relative vorticity at a grid point where the value is maximum over the low latitude Arabian Sea system

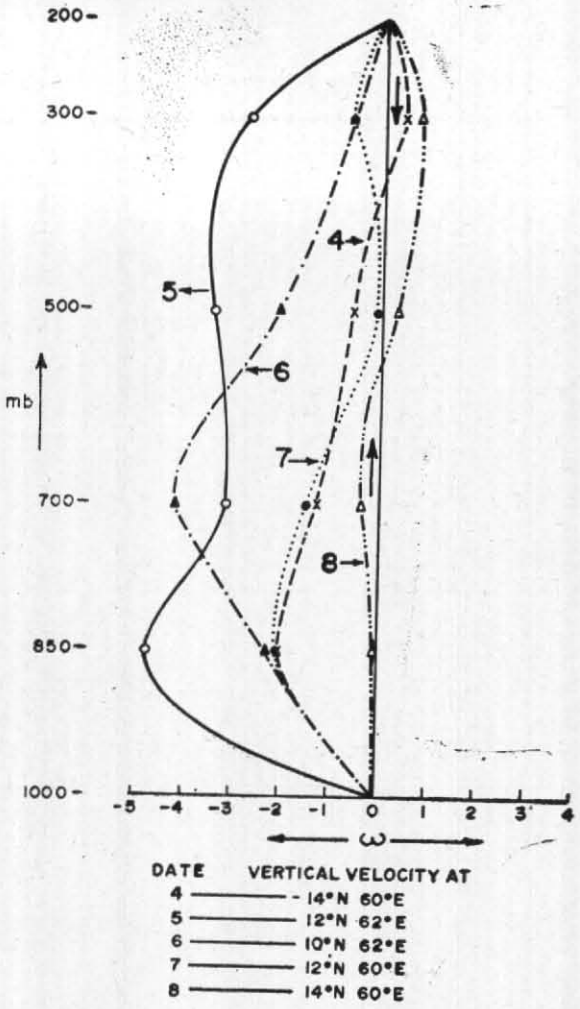

Fig. 8. Vertical profiles for vertical velocities at a grid point where the value is maximum over the low latitude Arabian Sea system

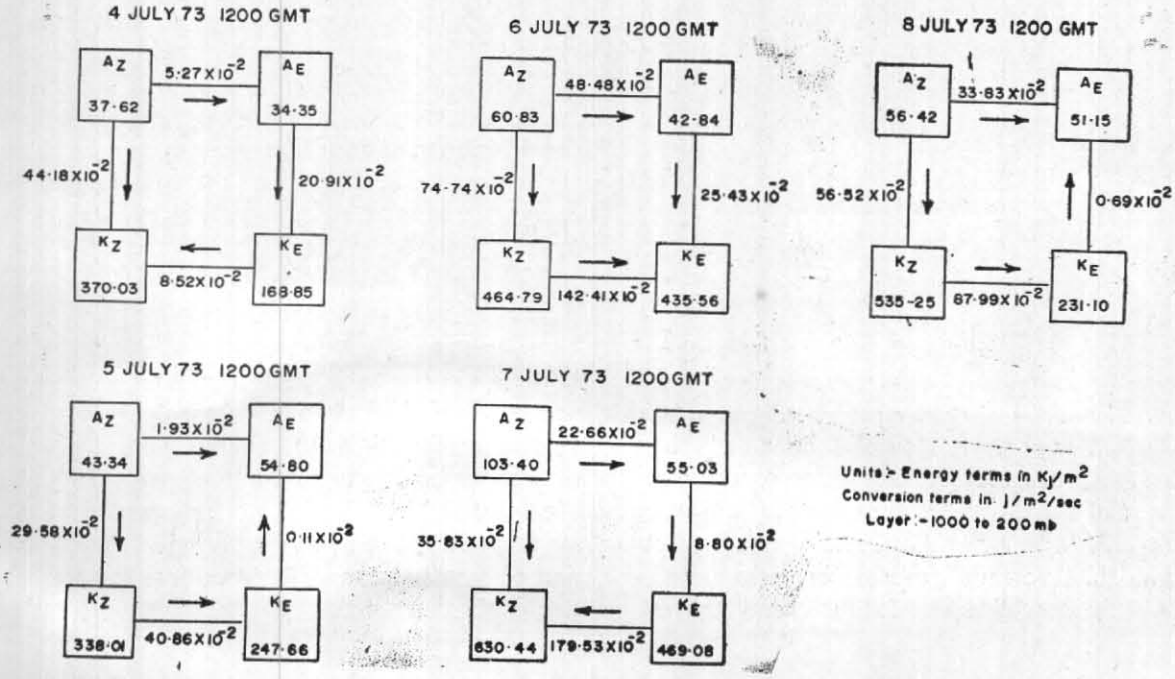

Fig. 9. Energy flow diagrams for 4 to 8 July 1973

TABLE 2

Energy terms for the layer 1000-200 mb from 4 to 8 July 1973, 1200 GMT

S.No.	Energy term	4 July	5 July	6 July	7 July	8 July	Units
1	A_Z	37·62	43·34	60·83	103·40	56·42	Kj/m^9
2	A_E	34·35	54·80	42·84	55·03	51·15	,,
3	K_Z	370·03	338·01	464·79	630·44	535·28	,,
4	K_E	168·85	247·66	435·56	469·08	231·10	,,
5	$\overline{u'v'}\ \frac{\partial \bar{u}}{\partial y}$	$8{\cdot}52\times10^{-2}$	$-40{\cdot}86\times10^{-2}$	$-142{\cdot}41\times10^{-2}$	$179{\cdot}53\times10^{-2}$	$-87{\cdot}99\times10^{-2}$	j/m^2/sec
6	$\frac{1}{\sigma}\left(\frac{R}{P}\right)^2 \overline{v'\ T'}\ \frac{\partial \bar{T}}{\partial y}$	$-5{\cdot}27\times10^{-2}$	$-1{\cdot}93\times10^{-2}$	$-48{\cdot}48\times10^{-2}$	$-22{\cdot}66\times10^{-2}$	$-33{\cdot}83\times10^{-2}$	,,
7	$\partial(\overline{\omega''\ \phi})''/\partial p$	$10{\cdot}38\times10^{-2}$	$4{\cdot}69\times10^{-2}$	$-2{\cdot}68\times10^{-2}$	$-1{\cdot}52\times10^{-2}$	$0{\cdot}12\times10^{-2}$	,,
8	$\overline{\omega''\ \partial\phi''}/\partial p$	$44{\cdot}18\times10^{-2}$	$29{\cdot}58\times10^{-2}$	$74{\cdot}74\times10^{-2}$	$35{\cdot}83\times10^{-2}$	$56{\cdot}52\times10^{-2}$	,,
9	$\partial\ (\overline{\omega'\ \phi'})/\partial p$	$1{\cdot}04\times10^{-2}$	$5{\cdot}23\times10^{-2}$	$-2{\cdot}94\times10^{-2}$	$-1{\cdot}78\times10^{-2}$	$-1{\cdot}00\times10^{-2}$	,,
10	$\overline{\omega'\ \partial\phi'}/\partial p$	$20{\cdot}91\times10^{-2}$	$-0{\cdot}11\times10^{-2}$	$25{\cdot}43\times10^{-2}$	$8{\cdot}80\times10^{-2}$	$-0{\cdot}69\times10^{-2}$	,,

1000 mb to 200 mb level are presented in Table 2 for the period 4th to 8th. It may be seen that both the zonal kinetic and eddy kinetic energy terms increase from 4th to maximum on 7th and decrease thereafter. It may be recalled that the depression intensified on the 6th and continued to be so on 7th and began to weaken from 8th. It is of interest to note that the average zonal kinetic and average eddy kinetic energies have increased over the entire domain.

It is seen that the available potential energy is smaller than the kinetic energy by about one order of magnitude. It may be relevant to mention that whereas Lorenz (1955) and other workers have evaluated the available potential energy on hemispherical basis, the value calculated here refers to a limited region. It may also be noted that Smith (1969) has also evaluated for a restricted region. Further, since tropospheric isentropic surfaces tend to be merely horizontal in the tropics the available potential energy becomes small. In Fig. 9 the flow diagrams for the energy conversion terms are presented. From 4th to 6th the direction in which the various energies are converted are proper, whereas on 7th the conversion takes place from eddy kinetic energy to zonal potential energy. On a comparison of the total value of the eddy kinetic energy on 7th and 8th, it is seen that the eddy kinetic energy has decreased considerably and from this we may conclude that the computation which shows that the eddy kinetic energy was converted to zonal kinetic energy, is correct.

Acknowledgements

The authors would like to express their gratefulness to Prof. Y.P. Rao, Director General of Observatories for his keen interest and valuable suggestions in conection with this work. They also like to thank Mr. T.D. Chacko for typing the manuscript, Mr. G.R. Kadam for his help in the collection of data and Mr. A.R. Murudkar for preparation of the diagrams.

REFERENCES

Lorenz, E. N.	1955	*Tellus*, 7, 2, pp. 157-167.
Miller, F. R. and Keshavamurty, R. N.	1965	Proc. Symp. Met. Results of I.I.O.E., India met. Dep., pp. 337-349.
Phillips, N. A.	1956	*Quart. J.R. met. Soc.*, **82**, 352, pp. 123-164.
Rao, K. V. and Rajamani, S.	1970	*Indian J. Met. Geophys.*, **21**, 2, pp. 187-194.
	1972	*Mon. Weath. Rev.*, **100**, 5, pp. 383-388.
	1972	*Indian J. Met. Geophys.*, **23**, pp. 525-530.
	1975	*Indian. J. Met. Hydrol. Geophys.*, **26**, 3, pp. 369-374.
Smith, P. J.	1969	*Tellus*, **21**, pp. 202-207.
Wiin-Nielsen, A., Brown, J. A. and Drake, M.	1963	*Ibid.*, **15**, 3, pp. 261-279.
Wiin-Nielsen, A.	1965	Tech. Note No. 66, World Meteorological Organization, Geneva.

APPENDIX I

List of symbols used

$\mathbf{V}$	Geostrophic wind velocity	∇^2	Laplacian operator
ζ	Relative geostrophic vorticity	$J(A, B)$	Jacobian operator
f_0	Standard value of the coriolis parameter	$\mathbf{k}$	Unit vector in the vertical
ϕ	Geopotential	u	Wind speed in the x-direction
z	Height of an isobaric surface	v	Wind speed in the y-direction
ψ	Stream function for the non-divergent component of velocity	$(\bar{\ })$	Zonal mean
		$(\ )'$	Deviation from zonal mean
		$[\ ]$	Area mean
$\omega = \frac{dp}{dt}$	Individual change of pressure	ϕ_1, ϕ_2	Latitudes limiting the area under study
σ	Static stability	a	Radius of earth
θ	Potential temperature	M	Mass of the atmosphere from 1000 mb to 200 mb over the area under study
α	Specific volume	β	Rossby parameter
∇	Isobaric gradient operator	$(\ )''$	Deviation from area mean

APPENDIX II

The vorticity equation and the thermodynamic equation for the mean zonal motion are

$$\frac{\partial}{\partial t}\nabla^2\bar{\psi} + \frac{\partial^2}{\partial y^2}\overline{\frac{\partial \psi'}{\partial x}\frac{\partial \psi'}{\partial y}} - f_0\frac{\partial \omega}{\partial p} = 0 \qquad (1)$$

$$\frac{\partial}{\partial t}\left(\frac{\partial \bar{\phi}}{\partial p}\right) + \frac{\partial}{\partial y}\left(\overline{v'\frac{\partial \phi'}{\partial p}}\right) + \sigma\bar{\omega} = 0 \qquad (2)$$

$$\text{where } \nabla^2\bar{\psi} = -\frac{\partial \bar{u}}{\partial y}\ ;\ \frac{\partial \bar{\phi}}{\partial p} = -\frac{R\bar{T}}{\bar{P}} \qquad (3)$$

If the equations (1) and (2) for the mean zonal motion are subtracted from the equation of the total motion, we get the vorticity equation and the thermodynamic energy equation for the perturbation as

$$\frac{\partial}{\partial t}\nabla^2\psi' + \bar{u}\frac{\partial}{\partial x}\nabla^2\psi' + \left(\beta - \frac{\partial^2 \bar{u}}{\partial x^2}\right)v' - f_0\frac{\partial \omega'}{\partial p} + \left(u'\frac{\partial}{\partial x}\nabla^2\psi' + v'\frac{\partial}{\partial y}\nabla^2\psi'\right)' = 0 \qquad (4)$$

$$\frac{\partial}{\partial t}\left(\frac{\partial \phi}{\partial p}\right)+\bar{u}\frac{\partial^2 \phi'}{\partial x\,\partial p}-f_0\frac{\partial \bar{u}}{\partial p}v'+\sigma\omega'+$$
$$+\left(u'\frac{\partial^2 \phi'}{\partial x\,\partial p}+v'\frac{\partial^2 \phi'}{\partial y\,\partial p}\right)'=0 \quad (5)$$

$$\frac{\partial}{\partial y}\nabla^2\bar{\psi}=-\frac{\partial^2 \bar{u}}{\partial y^2}\;;\;\frac{\partial^2 \phi}{\partial y\,\partial p}=-f_0\frac{\partial \bar{u}}{\partial p} \quad (6)$$

Multiplying equation (1) by $-\psi$ and equation (2) by $\frac{1}{\sigma}\frac{\partial \phi}{\partial p}$ and integrating throughout the horizontal domain under consideration, the equations for the kinetic energy and the potential energy of the mean zonal motion are obtained as

$$2\pi a^2\int_{\phi_1}^{\phi_2}\frac{\partial}{\partial t}Kz\cos\phi\,\partial\phi$$
$$=-2\pi a^2\int_{\phi_1}^{\phi_2}\overline{u'v'}\frac{\partial \bar{u}}{\partial y}\cos\phi\,\partial\phi-$$
$$-2\pi a^2\int_{\phi_1}^{\phi_2}\frac{\partial}{\partial p}(\bar{\phi}\,\bar{\omega})\cos\phi\,\partial\phi+$$
$$+2\pi a^2\int_{\phi_1}^{\phi_2}\bar{\omega}\frac{\partial \bar{\phi}}{\partial p}\cos\phi\,\partial\phi \quad (7)$$

$$2\pi a^2\int_{\phi_1}^{\phi_2}\frac{\partial}{\partial t}Pz\cos\phi\,\partial\phi=2\pi a^2\int_{\phi_1}^{\phi_2}\frac{1}{\sigma}\left(\frac{R}{P}\right)^2\times$$
$$\times\;\overline{v'T'}\frac{\partial \bar{T}}{\partial y}\cos\phi\,\partial\phi+$$
$$+2\pi a^2\int_{\phi_1}^{\phi_2}\bar{\omega}\frac{\partial \bar{\phi}}{\partial y}\cos\phi\,\partial\phi \quad (8)$$

The equations for the kinetic energy and the potential energy of the perturbation are similarly obtained by multiplying equation (4) by $-\psi'$ and (5) by $\frac{1}{\sigma}\frac{\partial \phi'}{\partial p}$

$$2\pi a^2\int_{\phi_1}^{\phi_2}\frac{\partial}{\partial t}K_E\cos\phi\,\partial\phi$$
$$=2\pi a^2\int_{\phi_1}^{\phi_2}\overline{u'v'}\frac{\partial \bar{u}}{\partial y}\cos\phi\,\partial\phi-$$
$$-2\pi a^2\int_{\phi_1}^{\phi_2}\frac{\partial}{\partial p}(\overline{\phi'\omega'})\cos\phi\,\partial\phi+$$
$$+2\pi a^2\int_{\phi_1}^{\phi_2}\omega'\overline{\frac{\partial \phi'}{\partial p}}\cos\phi\,\partial\phi \quad (9)$$

$$2\pi a^2\int_{\phi_1}^{\phi_2}\frac{\partial}{\partial t}P_E\cos\phi\,\partial\phi$$
$$=-2\pi a^2\int_{\phi_1}^{\phi_2}\omega'\overline{\frac{\partial \phi'}{\partial p}}\cos\phi\,\partial\phi-$$
$$-2\pi a^2\int_{\phi_1}^{\phi_2}\frac{1}{\sigma}\left(\frac{R}{P}\right)^2\overline{v'T'}\frac{\partial \bar{T}}{\partial y}\cos\phi\,\partial\phi \quad (10)$$

In the above four equations we have neglected all flux terms, making use of the following relation,

$$\iint J(A,B)=0 \quad (11)$$

If the equations (7) to (10) are integrated in the vertical, the resulting equations are

$$\frac{\partial}{\partial t}\int_M Kz\,dm=-\int_M\overline{u'v'}\frac{\partial \bar{u}}{\partial y}dm+$$
$$+\int_M\bar{\omega}\frac{\partial \bar{\phi}}{\partial p}\,dm \quad (12)$$

$$\frac{\partial}{\partial t}\int_M P_Z\,dm=\int_M\frac{1}{\sigma}\left(\frac{R}{P}\right)^2\overline{v'T'}\frac{\partial \bar{T}}{\partial y}\,dm-$$
$$-\int_M\bar{\omega}\frac{\partial \bar{\phi}}{\partial p}\,dm \quad (13)$$

$$\frac{\partial}{\partial t}\int_M K_E\,dm=\int_M\overline{u'v'}\frac{\partial \bar{u}}{\partial y}\,dm+$$
$$+\int_M\overline{\omega'\frac{\partial \phi'}{\partial p}}\,dm \quad (14)$$

$$\frac{\partial}{\partial t}\int_M P_E\,dm=-\int_M\frac{1}{\sigma}\left(\frac{R}{P}\right)^2\overline{v'T'}\frac{\partial \bar{T}}{\partial y}\,dm-$$
$$-\int_M\overline{\omega'\frac{\partial \phi'}{\partial p}}\,dm \quad (15)$$